

Molecular analog of multiferroics: Electric and magnetic field effects in many-electron mixed-valence dimers

Cristian Bosch-Serrano,¹ Juan M. Clemente-Juan,¹ Eugenio Coronado,^{1,*} Alejandro Gaita-Ariño,¹ Andrew Palii,^{2,*} and Boris Tsukerblat^{3,*}

¹*Instituto de Ciencia Molecular (ICMol), Universidad de Valencia, C/ Catedrático José Beltrán, 2, 46980-Paterna, Spain*

²*Institute of Applied Physics, Academy of Sciences of Moldova, Kishinev, Moldova*

³*Department of Chemistry, Ben-Gurion University of the Negev, P.O. Box 653, Beer-Sheva 84105, Israel*

(Received 5 May 2012; published 25 July 2012)

We show here that mixed-valence (MV) magnetic molecules with a significant electron delocalization are extremely sensitive to an external electric field. In particular, we focus on the symmetric many-electron MV binuclear complexes that are on the borderline between Robin and Day classes II and III. In these molecules, the double-exchange, which has been shown to lead to the ferromagnetic ground spin state, competes with the electric field, which tends to localize the spin, thus creating an electric dipole and stabilizing the spin states with lower multiplicities. This provides an efficient and easy way to control the ground spin state of the molecule through the double-exchange mechanism. Thus, we predict that the application of an external electric field will lead to a strong stepwise decrease of the magnetic susceptibility and to a simultaneous increase of the electric polarization. The reverse effect, consisting of a sharp decrease of the electric polarization under the action of an external magnetic field, is also predicted. The results demonstrate that MV dimers of this class can be regarded as single-molecule analogs of multiferroics with promising potential to create a functional magnetoelectric unit in one molecule.

DOI: [10.1103/PhysRevB.86.024432](https://doi.org/10.1103/PhysRevB.86.024432)

PACS number(s): 36.40.Cg, 75.30.Gw

I. INTRODUCTION

One current focus of interest in molecular spintronics is the use of electric fields or currents, instead of magnetic fields, to control the spin state of a molecule so as to achieve an all-electrical control of the nanodevice.¹ However, most of this work remains theoretical, and it was only very recently shown that a static electric field can induce spin-crossover in nanodevices formed by a single nanoparticle of ~ 10 nm, i.e., an order of magnitude larger than that of a single molecule.¹ As theoretical proposals, we should mention the use of electric fields to induce spin-crossover in single-ion molecules presenting valence-tautomerism,² or the application of coherent Landau-Zener transitions triggered by an electric pulse in mixed-valence (MV) systems polarized by a static electric field.³ A third possibility is that of electrically manipulating the spin of a magnetic molecule formed by two magnetic centers by acting on the exchange interaction between them.⁴ In these cases, the two centers can be used as spin qubits, providing thus an opportunity to develop electrically controlled two-qubit gates. A further development of this concept involves the use of a molecular triangle formed by three antiferromagnetically coupled spins (or, in general, a noncentrosymmetric molecule formed by interacting spins).⁵ In this particular case, a spin-electric coupling mechanism is predicted, which will allow long-distance controllable coupling and scalable spin qubits when these molecules are placed in a microwave cavity.⁵

In this paper, an alternative possibility is investigated that deals with the electric field control of the spin in magnetic MV clusters. These molecular systems are of current interest in areas as diverse as biochemistry and molecular magnetism (see Ref. 6 and references therein) and molecular spintronics (see Ref. 7 and references therein). They are composed of metal ions of the same element in two different oxidation states,

in such a way that the extra electrons can be delocalized over these metal sites through the double-exchange mechanism. Depending on the rate of this delocalization, the MV compound can be classified according to the Robin and Day scheme.⁸ If the extra electron is strongly trapped, the MV compound belongs to class I; when it is fully delocalized, the compound is assigned to class III. Between these two extremes, we face an intermediate case (class II) for which the system behaves as localized at low temperatures and as delocalized at high temperatures. The localization-delocalization phenomenon is determined by the relative strength of the electronic intercenter interaction (electron transfer), which promotes the electron delocalization, and the vibronic coupling (closely connected with the Markus reorganization energy), which tends to localize the electron. This phenomenon manifests itself in the features of the intervalence transfer absorption bands.^{6,9} As distinguished from the papers so far mentioned (Refs. 1–5), we consider a MV system for which the electric field is able to create a large electronic dipole moment that is governed by the strength of the double exchange and strongly affected by the vibronic coupling. In this context, it is also to be noted that the results discussed in this article are essentially based on the solution of the dynamic vibronic models, which differentiates this work from most of studies on this subject. This type of approach provides high accuracy for the evaluation of the observables and properly works when the adiabatic approximation loses its accuracy.

In this paper, we focus exclusively on binuclear MV clusters. When the extra electron in such systems is localized on one of the two sites, a considerable electric dipole moment appears. As a result, the MV dimers are expected to be extremely sensitive to the action of an external electric field, with this sensitivity being dependent on the degree of the electron delocalization. In fact, the electric field can

significantly change the intervalence band exhibited by a MV compound. Such an effect is referred to as the intervalence band Stark effect.¹⁰ This has been measured in a variety of MV dimers, both symmetric and asymmetric, inorganic and organic.¹⁰ It is reasonable to distinguish the one-electron MV dimers, in which the extra electron is delocalized over two spinless cores, from the magnetic (many-electron) MV dimers, which are formed by two magnetic cores and an itinerant spin (extra electron) delocalized over magnetic sites. Relevant examples of magnetic MV dimers include iron-sulfur clusters,¹¹ a Ni(II)-Ni(III) binuclear complex,¹² and a recently discovered V(II)-V(III) binuclear complex.¹³ As distinguished from the one-electron MV dimers, in magnetic MV species, the effect of the electric field is expected to be essentially spin-dependent due to the presence of the double-exchange interactions.¹¹ Moreover, in such systems, an electric field is expected to affect not only the intervalence transfer bands, but also the magnetic properties of MV dimers as a result of the crossover of the low-lying spin levels. While there are numerous studies of MV compounds based on the well-elaborated Stark spectroscopy, consideration of the ability of the electric field to produce the crossover of the spin levels in magnetic MV dimers represents an unexplored area, in spite of the fact that such effects seem to be quite interesting in molecular spintronics. Earlier work¹⁴ was based on the static model and therefore ignored the vibronic interaction, while the framework of the semiclassical adiabatic vibronic approach in general fails to correctly predict the ground state of the borderline class II/III MV compounds (see later herein).¹⁵ Finally, another study¹⁶ focused on the transport through a d^1 - d^2 MV dimer rather than on the effect of the electric field on the ground spin state.

In the present paper, we will discuss in detail the effects of an external electric field on the low-lying spin multiplets of symmetric magnetic MV dimers that are on the borderline between Robin and Day classes II and III (see also earlier communication¹⁷).

The reverse effect of the magnetic field on the electric polarization of such systems will be considered as well. Based on the analysis of these two effects, we argue that the magnetic MV dimers with moderate electron delocalization provide a unique possibility to control on a molecular level the spin degrees of freedom by applying an electric field with the simultaneous magnetic field control of charge degrees of freedom. Therefore, these systems can be regarded as single-molecule analogs of multiferroics.¹⁸ Multiferroic structures are explored for high-sensitivity alternating current (ac) magnetic field sensors and electrically tunable microwave devices such as filters, oscillators, and phase shifters in which the ferri-, ferro-, or antiferromagnetic resonance is tuned electrically instead of magnetically. A possibility to create a single-molecule multiferroic is in line with the present-day trend of nanoscience and nanotechnology to create a functional magnetoelectric unit in one molecule.

Throughout the paper, we discuss the effects of the electric and magnetic fields using the d^3 - d^2 dimer composed of high-spin metal ions as a model system in which the double exchange is operative. This choice is dictated by the fact that this cluster represents the simplest magnetic MV dimer in which, along with the ferromagnetic (maximal

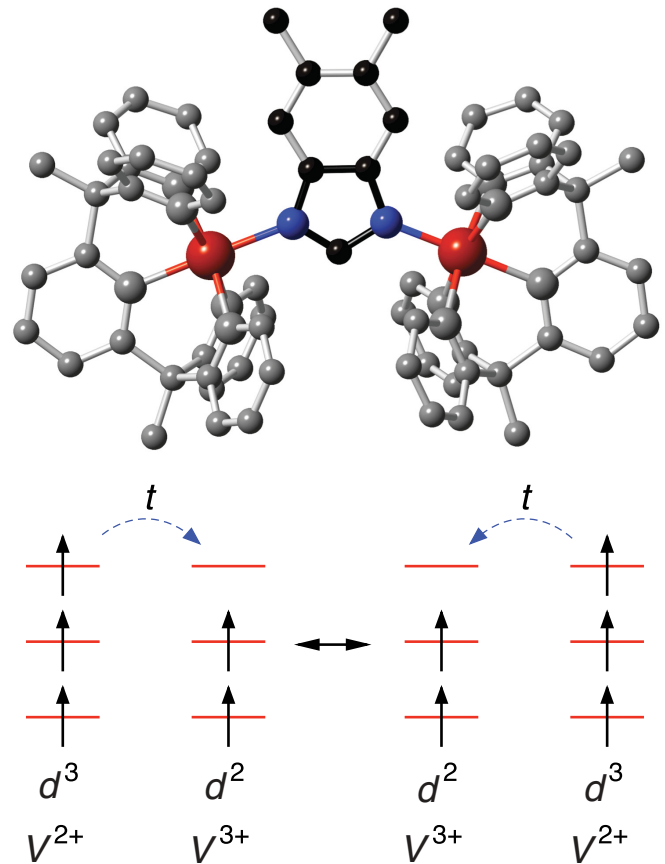


FIG. 1. (Color online) Schematic structure of a d^3 - d^2 MV dimer based on dinuclear vanadium complex and orbital scheme of the spin-dependent electron transfer (double exchange).

spin $S = 5/2$) and the antiferromagnetic (minimal spin $S = 1/2$) ground states, an intermediate spin value $S = 3/2$ can be stabilized under some special conditions. Additionally, a possible candidate for this experiment could be the recently reported¹³ MV dinuclear vanadium complex $\{[2,6\text{-bis}(1,1\text{-bis}(2\text{-pyridyl)ethyl)pyridine}]_2V_2(\mu\text{-}5,6\text{-dimethylbenzimidazolozate})\}(\text{PF}_6)_4$, which can be regarded as a d^3 - d^2 MV dimer exhibiting double exchange (see Fig. 1 and Ref. 13). In this complex, the ferromagnetic ground state with $S = 5/2$ was proved to be the result of the combined action of double exchange and vibronic coupling and was estimated to lie around 100 cm^{-1} below the $S = 3/2$ excited state.¹³ While this example serves as inspiration, the applicability of this work covers a wide variety of many-electron MV dimers. Besides the main electronic condition of borderline between Robin and Day classes II and III, one must take into account the structural condition that the bridging ligand is rigid. Larger distances between the two atoms hosting the “extra” electrons would of course mean a larger electric dipole and thus a higher sensitivity, but they would not actually be required because, as we will see, the electric field generated by current lasers applied on rather small molecules is more than enough to produce the effects we are studying.

II. THE MODEL

One can define the total Hamiltonian H_{tot} of the MV dimer in an external electric field as the dimer Hamiltonian in a zero electric field plus a dimer-field interaction term

$$H_{\text{tot}} = H_{\text{dim}} + H_{\text{dim-field}}. \quad (1)$$

The dimer term consists of an electronic part, a nuclear part, and an electronic-nuclear interaction term, as

$$H_{\text{dim}} = H_e + H_n + H_{e-n}. \quad (2)$$

The electronic term H_e includes the electron transfer (double exchange) and the Heisenberg-Dirac-Van-Vleck (HDVV) exchange contributions. The nuclear part H_n represents the free harmonic oscillator Hamiltonian. Finally, the term H_{e-n} describes the vibronic coupling between the extra electron and the nuclear vibrations.

In a basis of two localized electronic states, $\psi_A(S, M_S), \psi_B(S, M_S)$, the H_e -matrix is diagonal with respect to the quantum numbers S and M_S (total spin and its projection). In absence of the external magnetic field, the matrix elements are independent of M_S , and the matrix proves to have a block-diagonal structure for which each 2×2 block corresponds to a definite value of the total spin S . The 2×2 block $H_e(S)$ has the following form:

$$H_e(S) = -JS(S+1) + t_S \sigma_X, \quad (3)$$

where J is the HDVV exchange parameter, t_S is the transfer parameter, and σ_X is the Pauli matrix. In majority of cases, the HDVV exchange is antiferromagnetic, so $J < 0$.

When the extra electron is transferred over the spin cores formed by the localized electrons, the electron transfer is spin-dependent due to the double-exchange mechanism,¹⁹ with the effective (many-electron) spin-dependent transfer parameter being given by:

$$t_S = t(S+1/2)/(2s_0+1), \quad (4)$$

where t is the one-electron transfer integral, and s_0 is the spin of the core. The eigenvalues and the corresponding eigenvectors of the Hamiltonian, Eq. (3), are given by:

$$\begin{aligned} E_{\pm}(S) &= -JS(S+1) \pm t_S, \\ \psi_{\pm}(S, M_S) &= (1/\sqrt{2})[\psi_A(S, M_S) \pm \psi_B(S, M_S)]. \end{aligned} \quad (5)$$

The energy pattern of the MV dimer is independent of the sign of the transfer integral, and therefore for the sake of definiteness, we assume that t is positive. The ground eigenstate of the electronic Hamiltonian H_e results from the interplay of the two competing interactions: double exchange, which produces ferromagnetic effect, and antiferromagnetic HDVV exchange, which tends to stabilize the antiferromagnetic state.

In the systems that are on the borderline between Robin and Day classes II and III, the vibronic coupling is of crucial importance as it induces a trapping effect, which can lead to the localization of the extra electron at low temperatures and considerable reduction of the ferromagnetic double-exchange interaction. As a result, the spin in the ground state of the system is often smaller than that obtained with the electronic Hamiltonian H_e , so the effect of the vibronic interaction on the

spin states proves to be antiferromagnetic. The background for the consideration of vibronic effects in MV systems is represented by the vibronic model suggested by Piepho, Krausz, and Schatz (PKS model),²⁰ and it is widely used for the description of magnetic, spectroscopic, and conducting properties of many-electron MV dimers²¹ (see review article²² for more detailed bibliography). Being very efficient and, at the same time, relatively simple, the PKS model takes into account the most important features of the phenomenon. Within this model, the extra electron is assumed to interact only with the full-symmetric displacements Q_A and Q_B of the ligand surroundings of A and B ions (breathing modes). One can build the totally symmetric (in-phase) cluster mode Q_+ and antisymmetric (out-of-phase) mode Q_- cluster as follows:

$$Q_+ = (1/\sqrt{2})(Q_A + Q_B), \quad Q_- = (1/\sqrt{2})(Q_A - Q_B). \quad (6)$$

The out-of-phase mode Q_- is coupled to the electron motion, while the symmetric mode Q_+ can be excluded from the consideration. Therefore, we arrive at the one-mode vibronic problem. The important peculiarity of the PKS model is that only the ligands are involved in the active out-of-phase vibration, while the metals are assumed to be fixed, and thus the intermetallic distance $R_{AB} \equiv R$ remains constant in the course of nuclear motion. The vibronic interaction with the out-of-phase mode mixes the electronic states $\psi_+(S, M_S)$ and $\psi_-(S, M_S)$ separated by the gap $2t_S$, giving rise to the pseudo-Jahn-Teller effect.

The matrix of the total Hamiltonian H_{tot} in the basis of the electronic states $\psi_A(S, M_S), \psi_B(S, M_S)$ has a block-diagonal form, with each block of this matrix being related to a definite value of the total spin S :

$$\begin{aligned} H(S) &= \frac{\hbar\omega}{2} \left(q^2 - \frac{\partial^2}{\partial q^2} \right) \\ &\quad - JS(S+1) + (\nu q - d_0 E_Z) \sigma_Z + t_S \sigma_X. \end{aligned} \quad (7)$$

The first term in Eq. (7) represents the free harmonic oscillator Hamiltonian with the vibrational frequency ω for the out-of-phase mode, $q = \sqrt{M\omega/\hbar} Q_-$ is the corresponding dimensionless normal coordinate (M is the effective mass associated with the PKS vibration). The third term (containing Pauli matrix σ_Z) includes the linear vibronic interaction with the out-of-phase mode and the interaction of the electric dipole moment with the external electric field. In this term ν is the vibronic coupling parameter, $d_0 \sigma_Z$ is the matrix of the electric dipole moment operator d_Z , $d_0 = eR/2$ (e is the electron charge, and R is the distance between the metal sites A and B , which is typically 2–5 Å for metal clusters), and E_Z is the Z-component of the external electric field. Finally, the second and the last terms in Eq. (7) form the $H_e(S)$ -block of the electronic Hamiltonian, Eq. (3), and describe the antiferromagnetic HDVV exchange and the double exchange, respectively.

The two approaches are conventionally used for the vibronic interaction in MV systems, namely, the semiclassical adiabatic vibronic approximation,^{6,15,22} and a more exact quantum-mechanical approach based on the numerical solution of the dynamic vibronic problem.^{20,21} The two approaches

present a drastic discrepancy in prediction of the ground states in the special region in which $\frac{v^2}{\hbar\omega}$ is close to t and the minima of the adiabatic potentials with different S values are close in energy. In this case, the semiclassical adiabatic approximation loses its validity for the correct prediction of the ground state spin (see Appendix and Ref. 15). At the same time, this situation appears to be of special relevance for the present study, as in this case, an external electric field will be able to change the spin of the ground state. For this reason, we focus exclusively on the quantum-mechanical dynamic vibronic approach to study the effects of an electric field on the spin properties of these MV systems.

III. CONTROL OF THE LOCALIZATION-DELOCALIZATION AND THE SPIN STATE OF MV DIMERS BY APPLYING AN ELECTRIC FIELD: QUALITATIVE CONSIDERATIONS

The simplest MV cluster is represented by a symmetric one-electron MV dimer in which the unpaired electron is delocalized over two equivalent diamagnetic ions with spinless cores. The rate of the electron delocalization in such a system is governed exclusively by the interplay between the resonance interaction (one-electron transfer term of the Hamiltonian) and the vibronic interaction that couples the electronic motion with nuclear vibrations.²⁰ As it has been already mentioned in most cases the vibronic coupling tends to localize the extra electron (vibronic trapping effect), and so the electron transfer and the vibronic interaction prove to be in competition. As a result, in symmetric MV dimers, the rate of electron delocalization is determined by the relationship between the vibronic coupling parameter and the transfer parameter.²⁰ An important feature of a MV dimer is that it possesses a significant electric dipole moment, provided that the extra electron remains localized on one or another site. These electric dipole moments have equal absolute values (for symmetric MV dimers) and opposite directions. At the same time, such “localized” states cannot be regarded as the stationary states due to the existence of the transfer matrix element connecting two possible localizations of the extra electron. It follows from the equivalence of two possible orientations of the electric dipole moment that the expectation value of the electric dipole moment in any stationary state is vanishing; that is, a symmetric MV dimer cannot exhibit spontaneous electric polarization. However, this conclusion is valid only in the case of well-isolated MV dimers, when the electric dipole-dipole interaction between the neighboring dimers is not operative. On the contrary, in molecular crystals composed of symmetric MV dimers exhibiting strong cooperativity, the spontaneous electric polarization was proved to exist in the charge-ordered low-temperature phase, disappearing only at some critical temperature at which the structural phase transition occurs.²³ Here, we will not consider such a cooperative phenomenon and focus exclusively on the well-isolated MV dimers. In these, the nonzero electric dipole moment can appear only in the presence of an external electric field having a nonzero component along the axis connecting the two metal sites. Such ability of the electric field to polarize the system is due to the fact that the electric field leads to a “broken symmetry” for which two

possible orientations of the electric dipole moment become energetically nonequivalent. The induced electric polarization is crucially dependent on the degree of delocalization. Thus, when the extra electron is strongly delocalized (class III system), an electric field of reasonable magnitude is unable to produce any noticeable polarizing effect on the system. On the contrary, less delocalized systems (class II systems) are expected to be more sensitive to the applied electric field.

In contrast to the case of one-electron MV dimers, the extra electron in magnetic (many-electron) MV dimers is delocalized over the two spin cores (paramagnetic ions).²⁴ This leads to the emergence of new features, which significantly distinguish these systems from the one-electron ones. As was mentioned already, the most important feature of the magnetic MV dimers is that the localized spins in these systems are coupled through double exchange.¹⁹ This electronic interaction tends to stabilize the ferromagnetic state of the cluster and competes with the antiferromagnetic HDVV superexchange^{6,12,24} when the vibronic interaction is strong enough (compared to the transfer parameter). On the contrary, double exchange acts as a leading term when the degree of electron delocalization is large enough (i.e., in the weak vibronic coupling limit). In the intermediate case of moderate vibronic coupling (borderline class II/III), one can face the situation when the ground state is still ferromagnetic, but the gap between this state and the first excited state with smaller spin is relatively small, and an electric field can reverse the order of these spin states. As the high-spin state has more delocalized character, the low-spin state is more susceptible to undergo a charge separation and subsequent stabilization in the presence of an electric field. Therefore, an electric field will always have an antiferromagnetic effect favoring the stabilization of the lower spin states.

IV. CONTROL OF THE SPIN STATE OF A MAGNETIC MV DIMER BY APPLYING AN ELECTRIC FIELD: QUANTITATIVE CONSIDERATIONS

Figure 2 shows the low-lying vibronic spin levels calculated at $\hbar\omega = 200 \text{ cm}^{-1}$, $t = 2000 \text{ cm}^{-1}$, and $J = -100 \text{ cm}^{-1}$ as functions of the vibronic coupling parameter. The procedure of calculating of these levels is described in the Appendix. If the vibronic coupling is weak, the ground state possesses the maximal spin $S = 5/2$, while the first and second excited states have the spins $3/2$ and $1/2$, respectively. The increase of the vibronic coupling tends to trap the extra electron and thus to reduce the double exchange and, as a consequence, the spin of ground state. The change of the ground state spin from $S = 5/2$ to $S = 1/2$ occurs at the crossover value of the vibronic coupling constant $v_c \approx 700 \text{ cm}^{-1}$. Note that the intermediate spin state ($S = 3/2$) always remains an excited one for this set of the parameters.

Figure 3 demonstrates the effect of the electric field on the low-lying vibronic spin levels of the d^3-d^2 MV dimer calculated at the same values of $\hbar\omega$, t , and J as in Fig. 2 and for four different values of v satisfying the condition $v < v_c$. Under this condition, the ground state at zero electric field possesses the spin $S = 5/2$. This state remains the ground one under a weak electric field [left parts of the

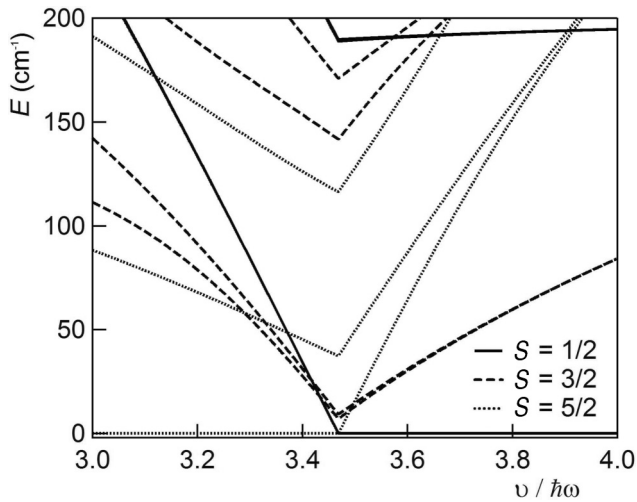
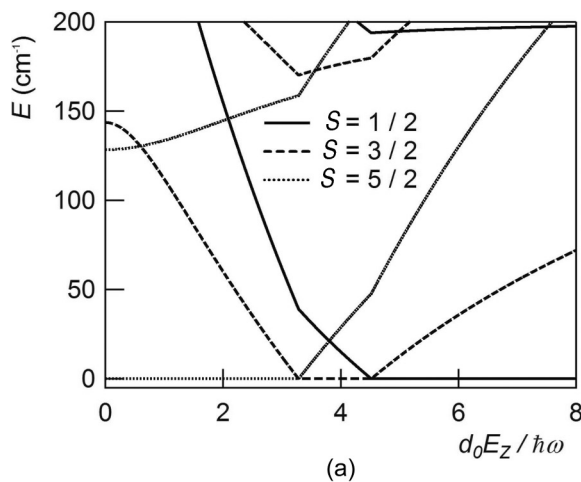


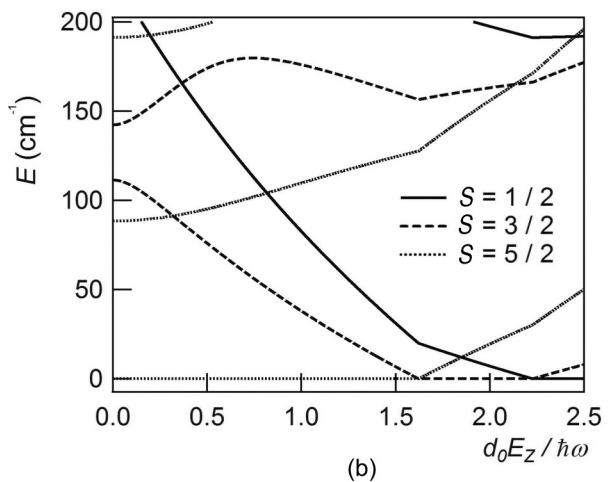
FIG. 2. Low-lying vibronic levels of the d^3-d^2 cluster calculated at $\hbar\omega = 200 \text{ cm}^{-1}$, $t = 2000 \text{ cm}^{-1}$, and $J = -100 \text{ cm}^{-1}$ as functions of the vibronic coupling parameter.

diagrams in Figs. 3(a), 3(b), 3(c), and 3(d)], but further increase of the electric field tends to stabilize the states

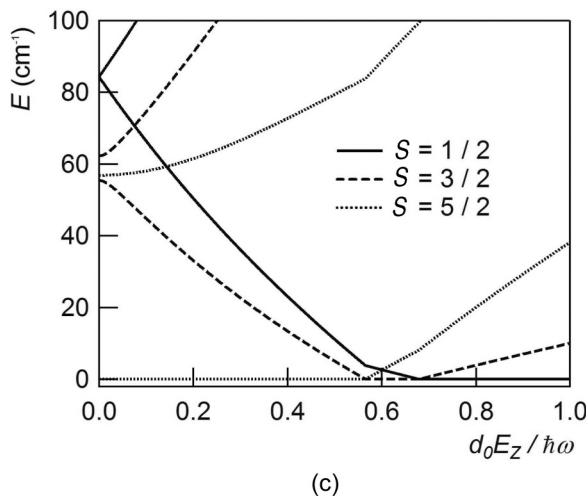
with smaller spin values. In fact, at some critical value of $d_0 E_Z$, a crossover of the low-lying vibronic spin levels is observed, which is accompanied by a decrease in the ground spin state. This antiferromagnetic effect of the electric field follows from the fact that this field tends to localize the extra electron, thus suppressing the ferromagnetic effect caused by the double exchange. The increase of the vibronic coupling parameter reduces the gap (at zero electric field) between the ferromagnetic ground state and the excited ones due to the vibronic suppression of the ferromagnetic double-exchange splitting. So, the stronger the vibronic coupling, the smaller is the critical value of $d_0 E_Z$ at which the crossover of the vibronic spin levels occurs. At weak vibronic coupling, the increase of the electric field gives rise to the two spin-crossover points [Figs. 3(a), 3(b), and 3(c)]: First, at moderate fields, the ground state changes from $S = 5/2$ to $S = 3/2$; then, at strong fields, it changes from $S = 3/2$ to $S = 1/2$. Note that the region of $d_0 E_Z$ for which the ground state corresponds to $S = 3/2$ is narrower for larger ν values [compare Figs. 3(a), 3(b), and 3(b)]; and finally, it fully disappears for strong enough vibronic coupling (when ν is close to ν_c) [Fig. 3(d)]. In this last case, we are dealing with a single crossover of the ground spin state from $S = 5/2$ to $S = 1/2$, without passing through an intermediate state with spin $S = 3/2$.



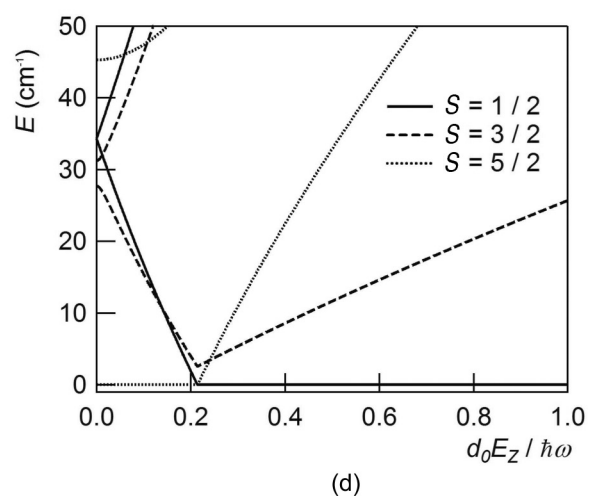
(a)



(b)



(c)



(d)

FIG. 3. Low-lying vibronic levels of the d^3-d^2 cluster as functions of the electric field calculated with $\hbar\omega = 200 \text{ cm}^{-1}$, $t = 2000 \text{ cm}^{-1}$, and $J = -100 \text{ cm}^{-1}$, and (a) $\nu = 500 \text{ cm}^{-1}$, (b) $\nu = 600 \text{ cm}^{-1}$, (c) $\nu = 660 \text{ cm}^{-1}$, and (d) $\nu = 680 \text{ cm}^{-1}$.

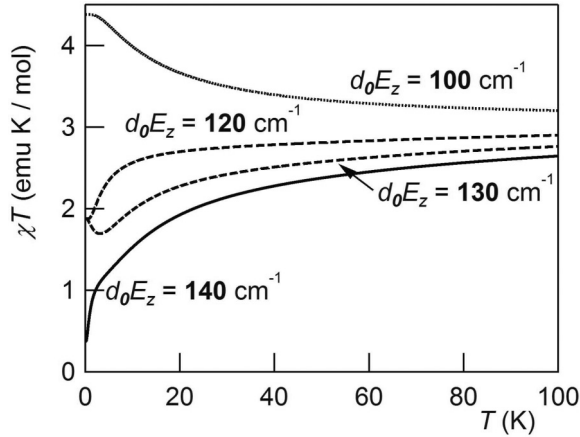


FIG. 4. Effect of the electric field on the temperature dependence of the magnetic susceptibility for the d^3 - d^2 MV dimer: $\hbar\omega = 200 \text{ cm}^{-1}$, $t = 2000 \text{ cm}^{-1}$, $J = -100 \text{ cm}^{-1}$, and $\nu = 660 \text{ cm}^{-1}$.

By using the Van Vleck equation, we have calculated the temperature dependence of the magnetic susceptibility (in the form χT vs T) under the application of an electric field for the same set of the parameters [Fig. 4]. Under a weak electric field (curve with $d_0 E_Z = 100 \text{ cm}^{-1}$ in Fig. 4), the ground state is ferromagnetic, and so we obtain $\chi T_{T \rightarrow 0} \approx 4.375 \text{ emu K/mol}$.

In the case of a moderate electric field, the intermediate spin state with $S = 3/2$ is stabilized (curves with $d_0 E_Z = 120 \text{ cm}^{-1}$ and 130 cm^{-1}), which corresponds to $\chi T_{T \rightarrow 0} \approx 1.875 \text{ emu K/mol}$. Finally, in the case of strong electric field (curve with $d_0 E_Z = 140 \text{ cm}^{-1}$), the ground state proves to be antiferromagnetic, and hence $\chi T_{T \rightarrow 0}$ takes the value of about 0.375 emu K/mol .

V. EFFECT OF THE ELECTRIC FIELD ON THE DIPOLE MOMENT OF A MAGNETIC MV DIMER

To evaluate the macroscopic dipole moment (electric polarization) induced by the applied electric field, one has to calculate first the extra electron densities ρ_A^v and ρ_B^v on the sites A and B in the v^{th} vibronic state with the total spin S (see Appendix). One finds

$$\begin{aligned} \rho_A^v(S) &= \sum_{n,n'} c_{n,v}^A(S) c_{n',v}^A(S) \int \Phi_n(q) \Phi_{n'}(q) dq \\ &= \sum_n [c_{n,v}^A(S)]^2, \\ \rho_B^v(S) &= \sum_n [c_{n,v}^B(S)]^2. \end{aligned} \quad (8)$$

With the aid of these expressions and the matrix representation $d_Z = d_0 \sigma_Z$ of the electric dipole moment operator, one obtains the following expression for the expectation value of the electric dipole moment in the vibronic state

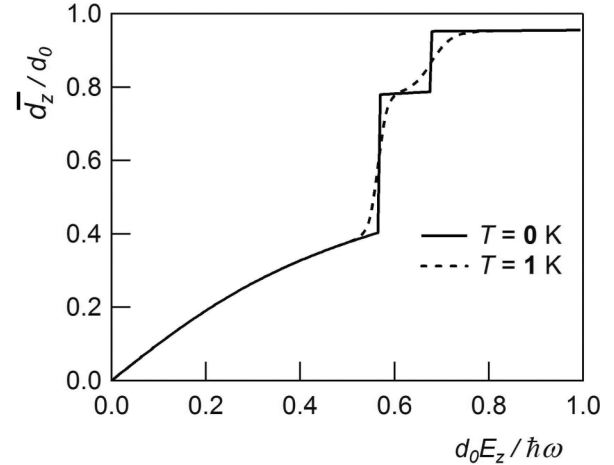


FIG. 5. Electric polarizations of the d^3 - d^2 cluster calculated as functions of the applied electric field with $\hbar\omega = 200 \text{ cm}^{-1}$, $t = 2000 \text{ cm}^{-1}$, $J = -100 \text{ cm}^{-1}$, and $\nu = 660 \text{ cm}^{-1}$ at temperatures 0 K and 1 K.

$\Psi_v(S, M_S)$:

$$\begin{aligned} \bar{d}_Z^v(S) &= \langle \Psi_v(S, M_S) | \hat{d}_Z | \Psi_v(S, M_S) \rangle = d_0 [\rho_A^v(S) - \rho_B^v(S)] \\ &= d_0 \sum_n \left\{ [c_{n,v}^A(S)]^2 - [c_{n,v}^B(S)]^2 \right\}. \end{aligned} \quad (9)$$

Finally, the macroscopic electric polarization is obtained as a statistical average over all vibronic states

$$\bar{d}_Z(T) = d_0 \frac{\sum_{v,S} \exp\left[-\frac{E_v(S)}{k_B T}\right] \sum_n [(c_{n,v}^A)^2 - (c_{n,v}^B)^2]}{\sum_{v,S} \exp\left[-\frac{E_v(S)}{k_B T}\right]}. \quad (10)$$

Figure 5 shows the dependencies of the electric polarization on the applied electric field calculated at zero temperature and at $T = 1 \text{ K}$ with the same set of $\hbar\omega$, t , J , and ν values as that used in the calculation of the dependence of the vibronic energy levels on $d_0 E_Z$ presented in Fig. 3(c). Since the MV dimer is symmetric, no electric polarization can appear at zero electric field.

The electric field induces electric polarization, which increases with the increase of the field. The important peculiarity of the \bar{d}_Z/d_0 vs $d_0 E_Z$ curve is its stair-step character, which appears due to the fact that the effect of the electric field strongly depends on the spin of the ground state. Note that the steps in the \bar{d}_Z/d_0 vs $d_0 E_Z$ curve are steep at low temperatures, while the steps are smoothed with increasing temperature (compare the curves with $T = 0$ and 1 K in Fig. 5). At the crossover of the lowest spin levels with $S = 5/2$ and $S = 3/2$, the delocalization diminishes, leading to a more sensitive outcome from the action of the electric field, as expected. As a result, the \bar{d}_Z value rapidly increases near this point, giving rise to a first step in the \bar{d}_Z/d_0 vs $d_0 E_Z$ curve. The second step corresponds to a crossover of the spin levels with $S = 3/2$ and $S = 1/2$. In general, every such spin level crossover will produce a step in both the electric dipole moment and the magnetization.

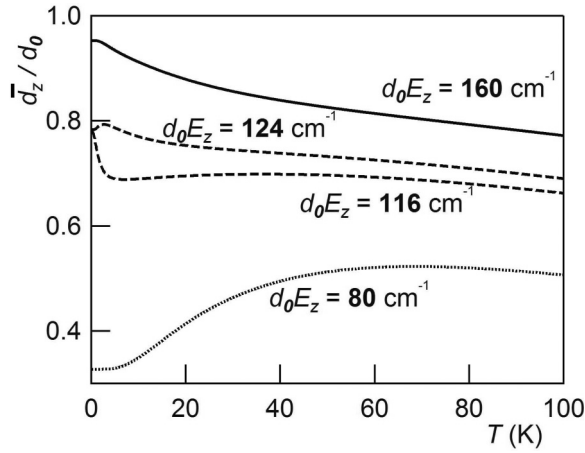


FIG. 6. Temperature dependencies of the electric polarization of the d^3 - d^2 cluster calculated at $\hbar\omega = 200 \text{ cm}^{-1}$, $t = 2000 \text{ cm}^{-1}$, $J = -100 \text{ cm}^{-1}$, and $\nu = 660 \text{ cm}^{-1}$ and with different values of the applied electric field.

Figure 6 shows the temperature dependencies of the electric polarization calculated at different values of the electric field, using the same set of parameters as in Figs. 3(c) and 5. At $d_0 E_Z = 80 \text{ cm}^{-1}$, when the ground state is ferromagnetic [Fig. 3(c)] and thus strongly delocalized, the electric polarization at low temperatures proves to be relatively small (around $0.33d_0$) [Fig. 6]. The first and second excited states possessing spins $S = 3/2$ and $1/2$ are less delocalized than the ground ferromagnetic state, and hence the temperature population of the excited levels results in the slow increase of \bar{d}_Z when the temperature is increased up to around 70 K. Providing $d_0 E_Z = 116 \text{ cm}^{-1}$ and 124 cm^{-1} , the ground state has an intermediate spin value $S = 3/2$ [Fig. 3(c)], and the \bar{d}_Z value is considerably higher as compared with that found at $d_0 E_Z = 80 \text{ cm}^{-1}$, when the ground state has $S = 5/2$. The different temperature behavior of \bar{d}_Z in the low-temperature region found for $d_0 E_Z = 116$ and 124 cm^{-1} is obviously due to the fact that the order of the excited vibronic levels in these two cases is opposite [Fig. 3(c)]. Finally, at $d_0 E_Z = 160 \text{ cm}^{-1}$, the ground vibronic level possesses $S = 1/2$, and hence the electric field is able to induce the high \bar{d}_Z value, while the population of the excited vibronic levels with larger spin gives rise to the decrease of \bar{d}_Z when the temperature is decreased [Fig. 6].

In general, the influence of the magnetic field on the electric polarization and the influence of the electric field on the magnetic moment can be expressed in terms of the magnetoelectric coupling coefficients, like $(\frac{\partial M}{\partial E})_{cr}$, which can be considered as useful quantities characterizing the system in the vicinity of the crossing of the vibronic levels where the magnetoelectric coupling is significant. As one can see, the effect is temperature dependent and maximal at $T = 0$, while an increase of the temperature leads to an effective decrease of the magnetoelectric coupling [Fig. 5]. It should also be noted that at very low temperature, the anisotropic exchange interactions become important as they result in the anticrossing of the vibronic levels belonging to different spin states, thus decreasing the magnetoelectric coupling. A more complete consideration of this issue will be given elsewhere.

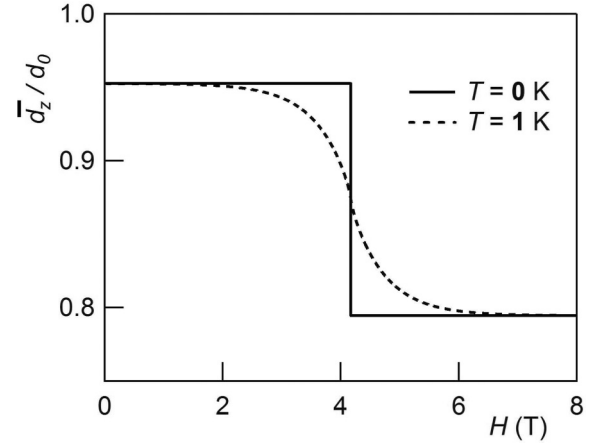


FIG. 7. Electric polarizations of the d^3 - d^2 cluster calculated as functions of the applied magnetic field with $\hbar\omega = 200 \text{ cm}^{-1}$, $t = 2000 \text{ cm}^{-1}$, $J = -100 \text{ cm}^{-1}$, $\nu = 660 \text{ cm}^{-1}$, and $d_0 E_Z = 160 \text{ cm}^{-1}$ at temperatures 0 K and 1 K.

VI. CONTROL OF THE ELECTRIC POLARIZATION OF A MAGNETIC MV DIMER BY APPLYING A MAGNETIC FIELD

In order to reveal the possibility to control the electric polarization by applying an external magnetic field, we will analyze the system corresponding to the upper curve in Fig. 6. At zero magnetic field, the ground state is antiferromagnetic ($S = 1/2$), the first excited level that is close in energy to the ground one possesses $S = 3/2$, and the second excited level has $S = 5/2$. In an applied magnetic field, these levels are split into Zeeman M_S sublevels, and at some critical value ($H_c \approx 4.15 \text{ T}$) of the magnetic field, the Zeeman sublevel with $M_S = -3/2$, arising from the first excited vibronic level with $S = 3/2$, becomes the ground one. Further increase of the magnetic field should lead to the second crossover, resulting in the stabilization of the ground Zeeman sublevel with $M_S = -5/2$, arising from $S = 5/2$. This, however, occurs (for the chosen set of parameters) at very strong magnetic fields. The electronic densities do not depend on M_S , and hence the expectation value of the electric dipole moment in the vibronic Zeeman state $\Psi_v(M_S)$ with given M_S should be exactly the same as that in the vibronic state $\Psi_v(SM_S)$ in a zero magnetic field. This leads to a stepwise decrease in polarization with increasing magnetic field as shown in Fig. 7. This decrease of \bar{d}_Z is evidently due to the fact that the state with $M_S = -3/2$, arising from $S = 3/2$, is more delocalized (and thus less sensitive to the action of the electric field) than the state with $M_S = -1/2$, arising from $S = 1/2$. Figure 8 displays the temperature dependencies of \bar{d}_Z/d_0 obtained at different values of the magnetic field. This figure allows us to understand better the role of the excited vibronic levels. Thus, at $H = 5 \text{ T}$, the first excited level with $M_S = -3/2$ arising from the level having $S = 3/2$ in zero magnetic field is close to the ground state, and hence even slight heating leads to the population of the first excited level. As a result, $\bar{d}_Z(H = 5 \text{ T})$ rapidly increases with the increase of temperature in the low-temperature region, reaches a maximum, and then goes down due to the population of the second excited level with $M_S = -1/2$, arising from the level

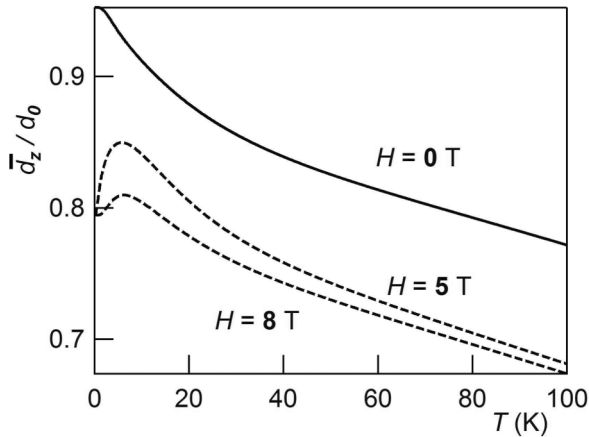


FIG. 8. Effect of the applied magnetic field on the temperature dependence of electric polarization calculated for the d^3-d^2 cluster with: $\hbar\omega = 200 \text{ cm}^{-1}$, $t = 2000 \text{ cm}^{-1}$, $J = -100 \text{ cm}^{-1}$, $\nu = 660 \text{ cm}^{-1}$, and $d_0 E_Z = 160 \text{ cm}^{-1}$.

having $S = 3/2$. At $H = 8 \text{ T}$, the low-temperature maximum is less pronounced, since, in this case, the gap between the ground and first excited Zeeman sublevels is larger as compared with the case of $H = 5 \text{ T}$.

It should be mentioned that by its physical nature, this effect of the magnetic field is similar to that predicted for charge-ordered MV crystals.²³ It should be noted that in Ref. 23, the cooperative effect is considered for the charge-ordered MV crystals, while the effect we discuss here is essentially molecular (zero-dimensional) in its nature.

In general, the MV systems for which the magnetoelectric coupling is expected to be strong should have closely spaced levels with different spin multiplicities. In this view, one should mention the study of the electronic structure of the MV $[\text{Re}_2\text{OCl}_{10}]^{3-}$ anion in Ref. 25. It was shown that the non-Hund states (producing an antiferromagnetic contribution to the double exchange) are rather close to the ground manifold. For this reason, the double exchange and the HDVV term become comparable to that shown²⁵ for the intermediate ground spin state. Under this condition, the systems with low energy of the non-Hund states (that is probably peculiar to the complexes of the heavy metal ions) can be sensitive to the external electric field. Of course, the last is also strongly influenced by the vibronic interaction, which should be additionally studied. It is worth mentioning that the degree of delocalization can be efficiently controlled by the length and conformation of the bridging ligands, as was discussed for the compounds with the spinless cores (see Ref. 3 and references therein). In particular, the longer bridge can significantly reduce the double exchange.

VII. CONCLUSIONS

In this paper, we show that delocalized MV magnetic clusters can provide ideal examples for an easy electric control of the spin state in a molecular system. Thus, we have theoretically investigated the effects of a static electric field on the magnetic behavior and electric polarization of symmetric many-electron MV binuclear complexes that are in the

borderline between class II and class III. Providing a moderate vibronic coupling and a dominant double exchange, as compared to the antiferromagnetic HDVV superexchange, the electric field has been shown to reduce the spin of the ground state. This leads to a sharp stepwise decrease in the magnetic susceptibility and a simultaneous increase in the electric polarization. We have also demonstrated that the electric polarization induced by the electric field can be considerably reduced by applying a magnetic field. The combination of these two reverse effects is somewhat similar to the magnetoelectric effect known for multiferroics²⁶ in which a magnetization (electric polarization) can be induced by applying an external electric (magnetic) field. In this context, the magnetic (many-electron) MV dimers belonging to the borderline class II-III can be regarded as single-molecule analogs of a multiferroic material with promising possibility to create a single-molecule functional magnetoelectric unit in one molecule.

In fact, in both classes of systems, the spin degree of freedom can be influenced by an electric field, while the charge degree of freedom proves to be sensitive to the action of a magnetic field. Obviously, the direct measurement of these effects constitutes a formidable challenge in molecular electronics that involves the study of single-molecule devices (i.e., on MV molecules connected to two or three electrodes), for which the electric transport through the molecule is expected to be dependent on its ground spin state. Still, in the short term, magnetic (electric) measurements in the presence of an electric (magnetic) field should be performed on molecular compounds formed by these magnetic MV dimers (preferably on single crystals with all dimers oriented along the same direction). These solid-state measurements should also include electron paramagnetic resonance measurements in presence of an electric field.

ACKNOWLEDGMENTS

Financial support from the EU (Project ELFOS and ERC Advanced Grant SPINMOL to E.C.), the Spanish MINECO (Project Consolider-Ingenio in Molecular Nanoscience, CSD2007-00010, and projects MAT2007-61584, and MAT2011-22785 co-financed by FEDER), and the Generalitat Valenciana (Prometeo Program) is gratefully acknowledged. C.B.-S. thanks the Spanish MEC for an FPU predoctoral grant. A.P. acknowledges the University of Valencia for a visiting research grant, and the STCU (project N 5062) and the Supreme Council on Science and Technological Development of Moldova for financial support. B.T. thanks the Israel Science Foundation (ISF) for financial support (Grant No. 168/09).

APPENDIX: COMPARISON OF VARIOUS VIBRONIC APPROACHES

In this Appendix, we focus on the case of zero electric field and compare the semiclassical adiabatic approach and the quantum-mechanical approach based on the numerical solution of the dynamic vibronic problem. In the adiabatic approximation, the nuclear kinetic energy is neglected, and

the full energy of the MV can be fully associated with the adiabatic potential. The two branches of the adiabatic potential corresponding to the total spin S are given by:

$$U_{\pm}^S(q) = -JS(S+1) + (\hbar\omega/2)q^2 \pm \sqrt{t_S^2 + v^2q^2}. \quad (\text{A1})$$

For $\frac{v^2}{\hbar\omega} > |t_S|$ (strong pseudo-Jahn-Teller effect), the lower sheet $U_{-}^S(q)$ of the adiabatic potential possesses two minima at the points

$$q_{\min}^{\pm}(S) = \pm \sqrt{\left(\frac{v}{\hbar\omega}\right)^2 - \left(\frac{t_S}{v}\right)^2}. \quad (\text{A2})$$

The system in the left (right) minimum is mainly localized on the site A (B), and the system belongs to the class II (moderate localization), in accordance with the Robin and Day classification scheme. On the contrary, for $\frac{v^2}{\hbar\omega} \leq |t_S|$ (weak pseudo-Jahn-Teller effect), the lower sheet possesses only one minimum at $q_{\min} = 0$ in which the system is fully delocalized (class III MV compound). Note that t_S increases with the increase of S , and hence one can face the situation when the condition for the existence of the localized minima is fulfilled for smaller S values, while for larger S values, the delocalized minima at $q_{\min} = 0$ do exist. The energy of the minima of the lower sheet of the adiabatic potential with the spin S is given by the following expression:

$$\begin{aligned} U_{-}^S[q = q_{\min}^{\pm}(S)] &= -JS(S+1) - \frac{v^2}{2\hbar\omega} - \frac{\hbar\omega}{2} \left(\frac{t_S}{v}\right)^2, \\ &\text{for } \frac{v^2}{\hbar\omega} > |t_S|, \\ U_{-}^S(q_{\min} = 0) &= -JS(S+1) - |t_S|, \\ &\text{for } \frac{v^2}{\hbar\omega} \leq |t_S|. \end{aligned} \quad (\text{A3})$$

Figure 9 shows the energies of the minima of the lower sheets of the adiabatic potentials with different spin values calculated for the d^3-d^2 cluster as functions of the dimensionless vibronic coupling parameter, providing strong (as compared with the HDVV exchange) double exchange. If the vibronic coupling is weak, the ground state possesses the maximal spin $S = 5/2$, while the first and second excited states have the spins $3/2$ and $1/2$, respectively.

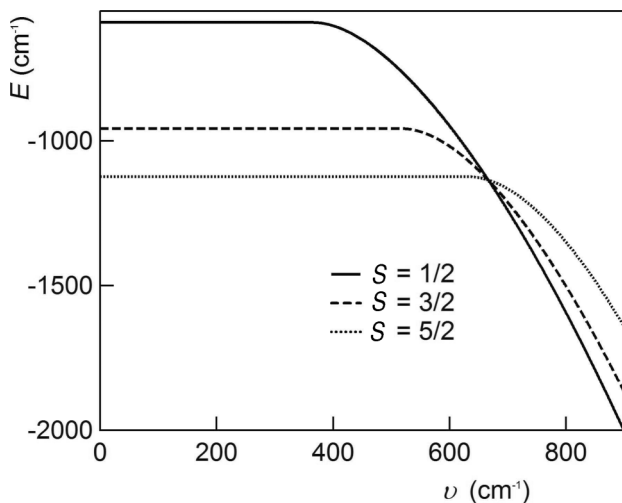


FIG. 9. Energies of the minima of the lower sheets of the adiabatic potential plotted for the d^3-d^2 MV dimer at $\hbar\omega = 200 \text{ cm}^{-1}$, $t = 2000 \text{ cm}^{-1}$, and $J = -100 \text{ cm}^{-1}$ as a function of the vibronic coupling parameter.

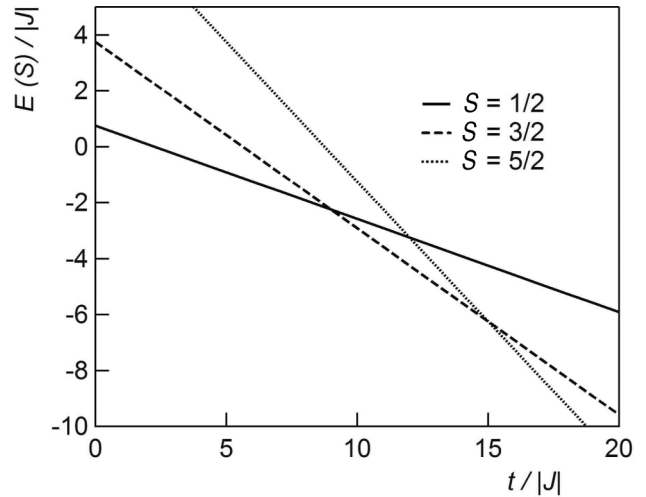


FIG. 10. Static correlation diagram for the d^3-d^2 cluster calculated with the aid of Eqs. (4) and (5).

culated for the d^3-d^2 cluster as functions of the dimensionless vibronic coupling parameter, providing strong (as compared with the HDVV exchange) double exchange. If the vibronic coupling is weak, the ground state possesses the maximal spin $S = 5/2$, while the first and second excited states have the spins $3/2$ and $1/2$, respectively.

The increase of the vibronic coupling tends to trap the extra electron and to reduce the double exchange, thus giving rise to a decrease of the gaps between the levels with $S = 5/2$, $3/2$, and $1/2$. One should expect that the increase of the vibronic coupling should produce the same effect on the ground state spin as the decrease of the double exchange in the static case, and hence the increase of v should result in the change of the ground state spin from $S = 5/2$ to $S = 3/2$ and then to $S = 1/2$, as occurs in the static correlation diagram [Fig. 10] upon decreasing the ratio $t/|J|$. Contrary to this intuitive concept, Fig. 9 shows that in the framework of the semiclassical adiabatic approach, the ground state can possess either $S = 5/2$ or $S = 1/2$ but not the state with intermediate spin $S = 3/2$. The crossover of the spin levels occurs at the following value of the vibronic coupling parameter:

$$v_c = \frac{t}{3} \sqrt{\frac{\hbar\omega}{2|J|}}. \quad (\text{A4})$$

At this point, the ground state proves to be degenerate with respect to the total spin value and comprises all S values. When $v > v_c$, the ground, first excited, and second excited levels possess the spin values $S = 1/2$, $3/2$, and $5/2$, respectively, in such a way that the order of the levels with $S = 1/2$ and $5/2$ is reversed as compared with that found for $v < v_c$. Note that the adiabatic semiclassical approach always leads to the conclusion about the inexistence of the ground state with an intermediate spin value.

Now let us proceed to a more comprehensive quantum-mechanical analysis of the vibronic effects based on the numerical solution of the dynamic vibronic problem. As distinguished from the adiabatic approximation, the

quantum-mechanical vibronic approach takes into account the kinetic energy of nuclear motion [term $-\frac{\hbar\omega}{2} \frac{\partial^2}{\partial q^2}$ in the Hamiltonian, Eq. (7)]. As a vibronic basis, we will use the products $\chi_n^A(S, M_S) \equiv \psi_A(S, M_S) \Phi_n(q)$ and $\chi_n^B(S, M_S) \equiv \psi_B(S, M_S) \Phi_n(q)$, where $\Phi_n(q)$ are the free harmonic oscillator wave functions ($n = 0, 1, 2, \dots$). This is the so-called weak coupling basis, when the harmonic oscillator's equilibrium position is at $q = 0$. The nonzero matrix elements of the total Hamiltonian in the vibronic basis $\chi_n^A(S, M_S)$, $\chi_n^B(S, M_S)$ are the following

$$\begin{aligned} & \langle \chi_n^A(S, M_S) | H_{\text{tot}} | \chi_n^A(S, M_S) \rangle \\ & \equiv -JS(S+1) - d_0 E_Z + \hbar\omega \left(n + \frac{1}{2}\right), \\ & \langle \chi_n^B(S, M_S) | H_{\text{tot}} | \chi_n^B(S, M_S) \rangle \\ & \equiv -JS(S+1) + d_0 E_Z + \hbar\omega \left(n + \frac{1}{2}\right), \\ & \langle \chi_n^A(S, M_S) | H_{\text{tot}} | \chi_n^B(S, M_S) \rangle = t_S, \\ & \langle \chi_n^A(S, M_S) | H_{\text{tot}} | \chi_{n+1}^A(S, M_S) \rangle \\ & = \langle \chi_{n+1}^A(S, M_S) | H_{\text{tot}} | \chi_n^A(S, M_S) \rangle = v\sqrt{(n+1)/2}, \\ & \langle \chi_n^B(S, M_S) | H_{\text{tot}} | \chi_{n+1}^B(S, M_S) \rangle \\ & = \langle \chi_{n+1}^B(S, M_S) | H_{\text{tot}} | \chi_n^B(S, M_S) \rangle = -v\sqrt{(n+1)/2}. \end{aligned} \quad (\text{A5})$$

The numerical diagonalization of this energy matrix gives the set of vibronic eigenvalues $E_\nu(S)$ and the corresponding eigenvectors

$$\begin{aligned} \Psi_\nu(S, M_S) &= \psi_A(S, M_S) \sum_n c_{n,\nu}^A(S) \Phi_n(q) \\ &+ \psi_B(S, M_S) \sum_n c_{n,\nu}^B(S) \Phi_n(q). \end{aligned} \quad (\text{A6})$$

Figure 11 shows the low-lying vibronic levels as a function of the vibronic coupling parameter calculated with the same t , J , and $\hbar\omega$ values as those used for the calculations of the minimal energies in the adiabatic approximation [Fig. 9]. By comparing Fig. 2 with Fig. 9, one can see that although

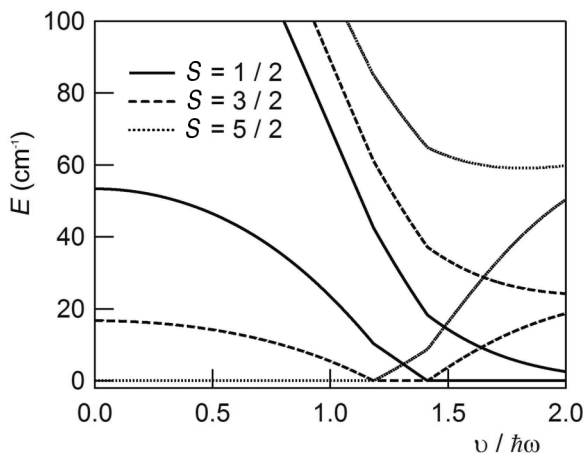


FIG. 11. Low-lying vibronic levels of the d^3-d^2 MV dimer calculated at $\hbar\omega = 200 \text{ cm}^{-1}$, $t = 200 \text{ cm}^{-1}$, and $J = -10 \text{ cm}^{-1}$ as a function of the vibronic coupling parameter.

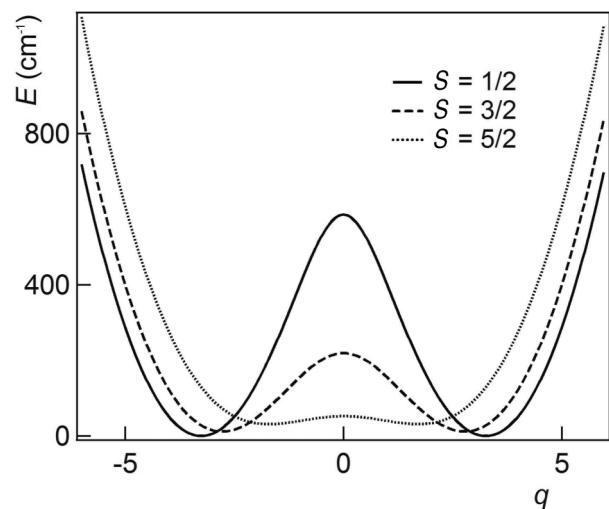


FIG. 12. Lower sheets of the adiabatic potential for the d^3-d^2 MV dimer at $\hbar\omega = 200 \text{ cm}^{-1}$, $t = 2000 \text{ cm}^{-1}$, $J = -100 \text{ cm}^{-1}$, and $\nu = 680 \text{ cm}^{-1}$.

both approaches predict the crossover of the spin levels with $S = 5/2$ and $S = 1/2$, the difference in critical values ν_c found within these two approaches is significant ($\nu_c \approx 667 \text{ cm}^{-1}$ in the semiclassical approach, while $\nu_c \approx 700 \text{ cm}^{-1}$ in the quantum-mechanical approach). Thus, for $\nu \approx 680 \text{ cm}^{-1}$, the adiabatic semiclassical approach predicts an antiferromagnetic ground state, $S = 1/2$ [Fig. 9], while the quantum-mechanical approach leads to the ferromagnetic one, $S = 5/2$ [Fig. 11]. This can be realized by inspecting the curvatures of the adiabatic potentials in the minima points and the barriers in Fig. 12. One can see that the curvature is maximal for the state with $S = 1/2$, and it is close to zero for the state with $S = 5/2$. As a result, the effective q -vibrational frequency proves to be higher for the antiferromagnetic ground state. It is also seen that the barrier for $S = 1/2$ is much higher than that for $S = 5/2$, and hence the tunneling splitting of the level with $n = 0$ is larger for higher S value. Therefore, in spite of the fact that $U_-^{1/2}[q = q_{\text{min}}^\pm(1/2)] < U_-^{5/2}[q = q_{\text{min}}^\pm(5/2)]$, the order of the low-lying vibronic levels is opposite, so that the ferromagnetic level proves to be the ground one for this set of parameters.

In addition, as distinguished from the semiclassical approach, which predicts that at $\nu = \nu_c$, the ground state comprises all spin values [Fig. 8], the quantum-mechanical approach predicts that the ground state includes only two spin values (maximal and minimal), while the state with intermediate spin value $S = 3/2$ proves to be the first excited one [Fig. 2(a)].

Even more drastic discrepancy between the two approaches can be found considering the special region in which $\frac{\nu^2}{\hbar\omega}$ is close to t . In this case, the quantum-mechanical approach predicts the existence of a region for the vibronic coupling parameter in which the ground state possesses an intermediate spin $S = 3/2$. This is in a strong contradiction with what has been shown from the semiclassical adiabatic approximation. Although the energy pattern in Fig. 11 is obtained with a particular set of parameters, it illustrates the inequivalence of the two approaches.

- *Corresponding authors: eugenio.coronado@uv.es, andrew.palii@uv.es, and tsuker@bgu.ac.il
- ¹S. Sanvito, *Chem. Soc. Rev.* **40**, 3336 (2011); F. Prins, M. Monrabal-Capilla, E. A. Osorio, E. Coronado, and H. S. J. van der Zant, *Adv. Mat.* **23**, 11545 (2011).
- ²A. Droghetti and S. Sanvito, *Phys. Rev. Lett.* **107**, 047201 (2011).
- ³J. M. Clemente-Juan, E. Coronado, A. V. Palii, and B. S. Tsukerblat, *J. Phys. Chem. C* **116**, 4999 (2012).
- ⁴N. Baadji, M. Piacenza, T. Tugsuz, F. Della Sala, G. Maruccio, and S. Sanvito, *Nat. Mater.* **8**, 813 (2009); J. Lehmann, A. Gaita-Ariño, E. Coronado, and D. Loss, *Nature Nanotech.* **2**, 312 (2007); *J. Mater. Chem.* **19**, 1672 (2009).
- ⁵M. Trif, F. Troiani, D. Stepanenko, and D. Loss, *Phys. Rev. Lett.* **101**, 217201 (2008).
- ⁶D. M. Brown, in *Mixed Valence Compounds* (D. Reidel, Dordrecht, The Netherlands, 1980); *Mixed Valence Systems: Applications in Chemistry, Physics and Biology*, NATO ASI Series 343, edited by K. Prassides (Kluwer Academic Publishers, Dordrecht, The Netherlands, 1991); G. Blondin and J. J. Girerd, *Chem. Rev.* **90**, 1359 (1990); J. J. Borrás-Almenar, J. M. Clemente-Juan, E. Coronado, A. V. Palii, and B. S. Tsukerblat in *Magnetoscience—From Molecules to Materials*, edited by J. Miller and M. Drillon (Wiley-VCH, 2001), pp. 155–210; K. D. Demadis, C. M. Hartshorn, and T. J. Meyer, *Chem. Rev.* **101**, 2655 (2001); D. M. D'Alessandro and F. R. Keene, *Chem. Soc. Rev.* **35**, 424 (2006); P. Day, N. S. Hush, and R. J. H. Clark, *Phil. Trans. R. Soc. A* **366**, 5 (2008); E. I. Solomon, X. Xie, and A. Dey, *Chem. Soc. Rev.* **37**, 623 (2008).
- ⁷A. Soncini, T. Mallah, and L. F. Chibotaru, *J. Am. Chem. Soc.* **132**, 8106 (2010).
- ⁸M. B. Robin and P. Day, *Adv. Inorg. Chem. Radiochem.* **10**, 247 (1967).
- ⁹N. S. Hush, *Prog. Inorg. Chem.* **8**, 391 (1967).
- ¹⁰J. R. Reimers, N. S. Hush in *Mixed Valence Systems: Applications in Chemistry, Physics and Biology*, NATO ASI Series 343, edited by K. Prassides (Kluwer Academic Publishers, Dordrecht, The Netherlands, 1991), p. 29; D. H. Oh, M. Sano, and S. G. Boxer, *J. Am. Chem. Soc.* **113**, 6880 (1991); B. S. Brunshwig, C. Creutz, and N. Sutin, *Coord. Chem. Rev.* **177**, 61 (1998); T. P. Treynor and S. G. Boxer, *J. Phys. Chem. A* **108**, 1764 (2004); P. Kanchanawong, M. G. Dahlbom, T. P. Treynor, J. R. Reimers, N. S. Hush, and S. G. Boxer, *J. Phys. Chem. B* **110**, 18688 (2006); L. N. Silverman, P. Kanchanawong, T. P. Treynor, and S. G. Boxer, *Phil. Trans. R. Soc. A* **366**, 33 (2008); L. F. Murga and M. J. Ondrechen, *J. Inorg. Biochem.* **70**, 245 (1998).
- ¹¹D. R. Gamelin, E. L. Bominaar, M. L. Kirk, K. Wieghardt, and E. I. Solomon, *J. Am. Chem. Soc.* **118**, 8085 (1996); D. R. Gamelin, E. L. Bominaar, C. Mathoniere, M. L. Kirk, K. Wieghardt, J.-J. Girerd, and E. I. Solomon, *Inorg. Chem.* **35**, 4323 (1996).
- ¹²A. Bencini, D. Gatteschi, and L. Sacconi, *Inorg. Chem.* **17**, 2670 (1978).
- ¹³B. Bechlars, D. M. D'Alessandro, D. M. Jenkins, A. T. Iavarone, S. D. Glover, C. P. Kubiak, and J. R. Long, *Nature Chem.* **2**, 362 (2010).
- ¹⁴B. S. Tsukerblat and B. D. Geikhman, *Sov. Phys. Solid State* **33**, 1931 (1991).
- ¹⁵J. J. Borrás-Almenar, E. Coronado, H. M. Kishenevsky, and B. S. Tsukerblat, *Chem. Phys. Lett.* **217**, 525 (1994).
- ¹⁶F. Reckermann, M. Leijnse, and M. R. Wegewijs, *Phys. Rev. B* **79**, 075313 (2009).
- ¹⁷C. Bosch-Serrano, J. M. Clemente-Juan, E. Coronado, A. Gaita-Ariño, A. Palii, and B. Tsukerblat, *Chem. Phys. Chem.* (2012), doi:10.1002/cphc.201200383.
- ¹⁸J. van den Brink and D. Khomskii, *J. Phys. Condens. Matter* **20**, 434217 (2008); D. I. Khomskii, *J. Magn. Magn. Mater.* **306**, 1 (2006); S.-W. Cheong and M. Mostovoy, *Nat. Mater.* **6**, 13 (2007); Y. Tokura, *J. Magn. Magn. Mater.* **310**, 1145 (2007); C. N. R. Rao and C. R. Serrao, *J. Mater. Chem.* **17**, 4931 (2007); W. Eerenstein, N. D. Mathur, and J. F. Scott, *Nature* **442**, 759 (2006); P. Garcia-Fernandez and I. B. Bersuker, *Phys. Rev. Lett.* **106**, 246406 (2011); A. Stroppa, P. Jain, P. Barone, M. Marsman, J. M. Perez-Mato, A. K. Cheetham, H. W. Kroto, and S. Picozzi, *Angew. Chem. Int. Ed.* **50**, 5847 (2011); I. B. Bersuker, *Phys. Rev. Lett.* **108**, 137202 (2012).
- ¹⁹C. Zener, *Phys. Rev.* **82**, 403 (1951); P. W. Anderson and H. Hasegawa, *ibid.* **100**, 675 (1955).
- ²⁰S. B. Piepho, E. R. Krausz, and P. N. Schatz, *J. Am. Chem. Soc.* **100**, 2996 (1978); K. Y. Wong and P. N. Schatz, *Prog. Inorg. Chem.* **28**, 369 (1981).
- ²¹S. A. Borshch, I. N. Kotov, and I. B. Bersuker, *Chem. Phys. Lett.* **111**, 264 (1984); B. S. Tsukerblat, H. M. Kishinevsky, A. V. Palii, V. Ya. Gamurar, and A. S. Berengolts, *Mol. Phys.* **76**, 1103 (1992); A. V. Palii, M. I. Belinsky, and B. S. Tsukerblat, *Chem. Phys.* **255**, 51 (2000).
- ²²B. Tsukerblat, S. Klokishner, and A. Palii, in *The Jahn–Teller Effect. Fundamentals and Implications for Physics and Chemistry*, Springer Series in Chemical Physics, edited by H. Köppel, D. R. Yarkony, and H. Barentzen (Springer, Heidelberg, Dordrecht, London, New York, 2009), Vol. 97, pp. 555–620.
- ²³S. I. Klokishner and B. S. Tsukerblat, *Chem. Phys.* **125**, 11 (1988); A. V. Koryachenko, S. I. Klokishner, and B. S. Tsukerblat, *ibid.* **150**, 295 (1991); B. S. Tsukerblat, S. I. Klokishner, and B. L. Kushkuley, *ibid.* **166**, 97 (1992); S. Klokishner, K. Boukheddaden, and F. Varret, *Phys. Rev. B* **60**, 150 (1999); S. I. Klokishner and O. S. Reu, *Phys. Status Solidi B* **234**, 611 (2002).
- ²⁴M. I. Belinskii, B. S. Tsukerblat, and N. V. Gerbeleu, *Sov. Phys. Solid State* **79**, 497 (1983); L. Noodelman and E. J. Baerends, *J. Am. Chem. Soc.* **106**, 2316 (1984); V. Papaefthymiou, J.-J. Girerd, I. Moura, J. J. G. Moura, and E. Münck, *ibid.* **109**, 4703 (1987); M. Drillon, G. Pourroy, and J. Darriet, *J. Chem. Phys.* **88**, 27 (1984); S. A. Borshch, I. N. Kotov, and I. B. Bersuker, *Sov. J. Chem. Phys.* **3**, 1009 (1985).
- ²⁵N. Guihéry, *Theor. Chem. Acc.* **116**, 576 (2006).
- ²⁶Y. Tokura and S. Seki, *Adv. Mater.* **22**, 1554 (2010).